Constructing a Continuous Parameter Range of Computational Flows

H. Thomas Sharp* and L. Sirovich†
Brown University, Providence, Rhode Island

Flow past a body, in general, is specified by a variety of parameters such as thickness, angle of attack, camber, Mach number, as well as others. A particular flow, therefore, is characterized by a single point in the corresponding parameter space. Conversely, the numerical calculation of a particular flowfield yields information at just one point of the parameter space. However, the nature of a continuous range of nearby flowfields is of fundamental significance in the design and performance of aircraft. To treat this generally, one can consider the variational equations (which are linear) obtained by differentiating the exact equations with respect to each of the relevant parameters. The resulting matrix of derivatives of flow quantities is referred to as the Jacobi matrix. The subsequent procedure is in principle now straightforward. One integrates the nonlinear governing equations—which results in the determination of just one point in parameter space—and simultaneously the variational equations governing the Jacobi matrix. The last then is used to describe the neighborhood of the already determined point of the parameter space. Because the variational equations are linear, the additional computational time required for their integration is modest.

I. Problem

FREQUENTLY, when calculating the flow about a body, one is interested in how the flow will change if the base configuration is altered. For example, one may want to know what will happen at a slightly different angle of attack, wing loading, camber, or thickness. To answer such questions, each parameter change is traditionally considered as a separate case, and flow simulation code is repeatedly run. It could be argued, quite effectively, that in many instances this is not an efficient use of resources. Why undertake an entirely new calculation of the flow when we know the results at a nearby state? A method is presented herein that allows efficient generation of solutions in the neighborhood of a base solution.

II. Introduction

In general terms, we consider a system of nonlinear partial differential equations

$$\boldsymbol{F}(\boldsymbol{u}(\boldsymbol{x}, \ldots; \boldsymbol{\epsilon}), \boldsymbol{x}, \ldots; \boldsymbol{\epsilon}) = 0 \tag{1}$$

in the flow variables $\boldsymbol{u}$, dependent variables $\boldsymbol{x}$, and parameters $\boldsymbol{\epsilon}$. For purposes of exposition, we consider $\boldsymbol{u}(\boldsymbol{x}; \boldsymbol{\epsilon})$ as known and seek the solution at a neighboring point in parameter space. The parametrically differentiated dependent variables are governed by the equations obtained by differentiating Eq. (1), namely,

$$\frac{\mathrm{d}}{\mathrm{d}\epsilon_k} F_i(u, x, \ldots; \epsilon) = \frac{\partial F_i}{\partial u_j}\frac{\partial u_j}{\partial \epsilon_k} + \frac{\partial F_i}{\partial \epsilon_k} = 0 \tag{2}$$

Thus, in general, on-square matrix $\partial u_i/\partial \epsilon_k$ is known as the Jacobi matrix, and the above procedure provides a linear system of equations governing the Jacobi matrix. The term $\partial F_i/\partial u_j$ actually represents an operator, the details of which are best left to the individual cases. If $u^0 = u(x; \epsilon_0)$ represents a known solution of the flow, then any neighboring flow at some fixed point x is determined by

$$\boldsymbol{u}(\boldsymbol{x}; \boldsymbol{\epsilon}) = \boldsymbol{u}^0 + \frac{\partial \boldsymbol{u}^0}{\partial \boldsymbol{\epsilon}_k}(\boldsymbol{\epsilon}_k - \boldsymbol{\epsilon}_0) \tag{3}$$

A basic difficulty with what has just been said, in particular with the use of Eq. (3), is the fact that because the description of the body may depend on ϵ, the conditions on the problem may occur at locations that vary with ϵ. Specifically, both the boundary locations and the shock locations will generally vary with changes in the parameters ϵ. The method presented avoids the difficulties implicit with such spatial variations in ϵ.

III. Application to Two-Dimensional Flow

To illustrate this method, we consider steady, inviscid, supersonic flows past two-dimensional airfoils. For this purpose, consider a family of profiles depending on three parameters (thickness, camber, and angle of attack). For completeness, we summarize the methods used in solving such flows.[1,2] The equations are written in characteristic form as follows:

$$s_\beta = 0 \tag{4}$$

$$[\theta + P(\mu)]_\alpha = \frac{\sin 2\mu}{2\alpha}\frac{\mathrm{d}s}{\mathrm{d}\alpha} \tag{5}$$

$$[\theta - P(\mu)]_\beta = (1 - \tan\theta \tan\mu)\frac{x_\beta}{x_\alpha}\theta_\alpha \tag{6}$$

Here, the coordinates (α, β) correspond to the streamlines, $\alpha = \text{const}$, and the $C+$ characteristics, $\beta = \text{const}$ (Fig. 1); θ is the flow-deflection angle, μ the Mach angle, and s the entropy. (The subscripts denote differentiation.) The Prandtl function $P(\mu)$ is given by

$$P(\mu) = \lambda^{1/2}\tan^{-1}(\lambda^{1/2}\tan\mu) - \mu, \qquad \lambda = (\gamma+1)/(\gamma-1) \tag{7}$$

An advantage to solving the above characteristic form of the equations is that it generates a body-fit, shock-fit coordinate

Received Feb. 20, 1987; revision received Nov. 15, 1988.

*Research Assistant, Division of Applied Mathematics; currently, Senior Aerodynamics Engineer, Lockheed Aeronautical Systems Co., Burbank, CA. Member AIAA.

†Professor, Division of Applied Mathematics.

system. We mention in passing that because the equations are exact, they are valid in the hypersonic flow regime so long as such real-gas effects as disassociation and ionization can be ignored.

The physical coordinates x, y satisfy the relations[1,2]

$$y_\alpha = x_\alpha \tan(\theta + \mu), \qquad y_\beta = x_\beta \tan\theta \tag{8}$$

The transformation to (α, β) coordinates leaves open two arbitrary functions, and these are fixed so that the shock is positioned along the line $\alpha = \beta$ and the airfoil is along $\alpha = 0$ (Fig. 2). Appropriate boundary conditions at the body are

$$x(0, \beta) = \beta, \quad y(0, \beta) = f(\beta, \epsilon), \quad \theta(0, \beta) = \tan^{-1}[f_\beta(\beta), \epsilon] \tag{9}$$

The Rankine–Hugoniot conditions govern the jumps in θ, μ, and s at the shock. Written in terms of the shock angle η (with $\gamma = 1.4$), they are given by

$$\tan\theta = \frac{1}{\tan\eta} \times \frac{(M^2 - 1)\tan^2\eta - 1}{\left[\left(1 + \frac{\gamma+1}{2}M^2\right) + \left(1 + \frac{\gamma-1}{2}M^2\right)\tan^2\eta\right]} \tag{10}$$

$$\sin^2\mu = \frac{0.2(1 + \frac{7}{6}w)(1 + \frac{1}{6}w)}{(1 + w)(1 + 0.2\,M^2) - (1 + \frac{7}{6}w)(1 + \frac{1}{6}w)} \tag{11}$$

$$s = 2.5\ell n(1 + \tfrac{7}{6}w) + 3.5\,\ell n(1 + \tfrac{1}{6}w) - 3.5\,\ell n(1 + w)$$

where

$$w = M^2 \sin^2\eta - 1 \tag{12}$$

The shock angle is related to the coordinates as follows:

$$\tan\eta = \left.\frac{dy}{dx}\right|_{\text{shock}} = \left.\frac{y_\alpha + y_\beta}{x_\alpha + x_\beta}\right|_{\text{shock}} \tag{13}$$

In the above, we have assumed a perfect gas with constant specific heats and hence that

$$p = p^\gamma \exp[(\gamma - 1)s] \tag{14}$$

It should be noted that this formulation eliminates the difficulty mentioned in the Introduction. For by using the (a, β)-coordinate system, a quantity such as

$$\frac{\partial p}{\partial \epsilon}(\alpha, \beta; \epsilon)$$

signifies the variation with ϵ at fixed α and β. In particular, it gives the variation of pressure, for example, fixed at the body or at the shock. This makes the integration of the differential equations significantly simpler.

IV. Variational Equations

We are interested in solutions to these equations at points near a known solution. To pursue this, we differentiate all of the above equations with respect to the parameter of interest. In keeping with the remarks at the close of the previous section, we emphasize that differentiation is with respect to ϵ with α and β held fixed.

The mechanics of the differentiation are straightforward but tedious. With one exception, we represent the differentiated variables by capitalized variables

$$\Theta = \frac{\partial\theta}{\partial\epsilon}, \quad S = \frac{\partial s}{\partial\epsilon}, \quad X = \frac{\partial x}{\partial\epsilon}, \quad Y = \frac{\partial y}{\partial\epsilon}, \quad \Psi = \frac{\partial\mu}{\partial\epsilon} \tag{15}$$

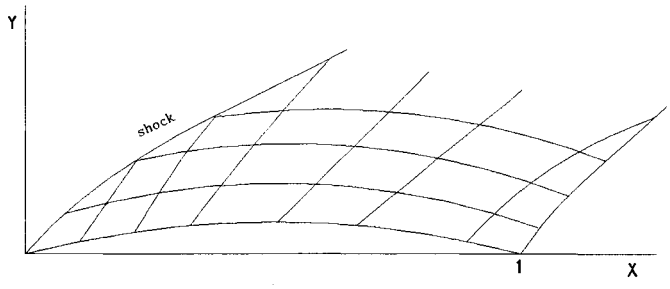

Fig. 1 Body, $C+$ and $C-$ characteristics in physical (x, y) plane.

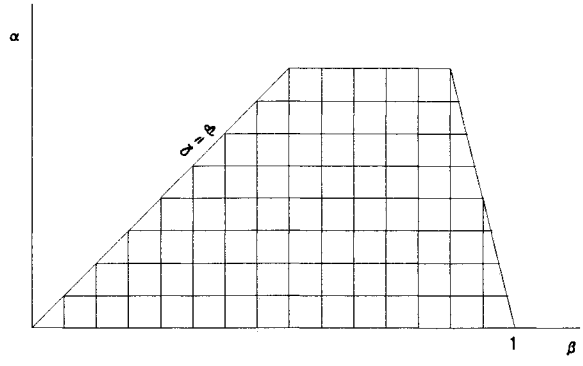

Fig. 2 Body, $C+$ and $C-$ characteristics in (α, β) plane.

When Eqs. (4–6) and (8) are parametrically differentiated, we then obtain

$$S_\beta = 0 \tag{16}$$

$$\Theta_\alpha + \left[P_{\mu\mu}(u)\mu_\alpha - \frac{s_\alpha \cos 2\mu}{\gamma}\right]\Psi + P_\mu(\mu)\Psi_\alpha - \frac{\sin 2\mu}{2}S_\alpha = 0 \tag{17}$$

$$\Theta_\beta + \frac{x_\beta\theta_\alpha}{x_\alpha}\sec^2\theta\,\tan\mu\Theta - (1 - \tan\theta\,\tan\mu)\frac{x_\beta}{x\alpha}\Theta_\alpha = P_\mu(\mu)\Psi_\beta + \left[P_{\mu\mu}(\mu)\mu_\beta - \frac{x_\beta\theta_\alpha}{x_\alpha}\sec^2\mu\,\tan\theta\right]\Psi + (1 - \tan\theta\,\tan\mu)\frac{\theta_\alpha}{x_\alpha}\left(X_\beta - \frac{x_\beta}{x_\alpha}X_\alpha\right) \tag{18}$$

$$Y_\alpha = X_\alpha \tan(\theta + \mu) + X_\alpha \sec^2(\theta + \mu)(\Theta + \Psi) \tag{19}$$

$$Y_\beta = X_\beta \tan\theta + X_\beta \sec^2\theta \tag{20}$$

It should be noted that we have dropped the specification that ϵ be a vector. This has been done for ease of exposition. This can be done without loss of generality. Variation with respect to each parameter can be treated separately, since only first-order variations are being considered. At the shock, the parametrically differentiated equations are (again with $\gamma = 1.4$)

$$\frac{d\eta}{d\epsilon} = \frac{\cos^2\eta}{(x_\alpha + x_\beta)^2}[Y_\alpha(x_\alpha + x_\beta) + Y_\beta(x_\alpha + x_\beta) - X_\alpha(y_\alpha + y_\beta) - X_\beta(y_\alpha + y_\beta)] \tag{21}$$

$$S = \left[\frac{17.5}{6 + 7w} + \frac{3.5}{6 + w} - \frac{3.5}{1 + w}\right]\frac{dw}{d\epsilon} \tag{22}$$

$$\Psi = \frac{0.2A(\frac{4}{3} + \frac{7}{18}w) - 0.2(1 + \frac{7}{6}w)(1 + \frac{1}{6}w)(0.2M^2 - \frac{1}{3} - \frac{7}{18}w)}{A^2 \sin 2\mu}\frac{dw}{d\epsilon} \tag{23}$$

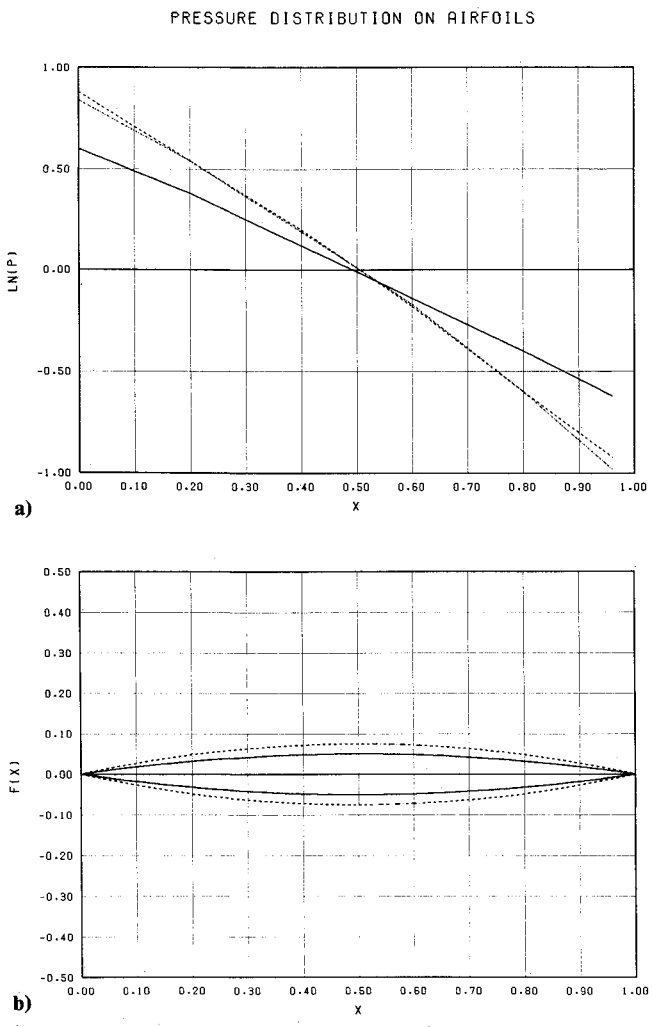

Fig. 3 a) Pressure distribution on 10% and 15% thick airfoils at $M = 2$; and b) 10% and 15% airfoils.

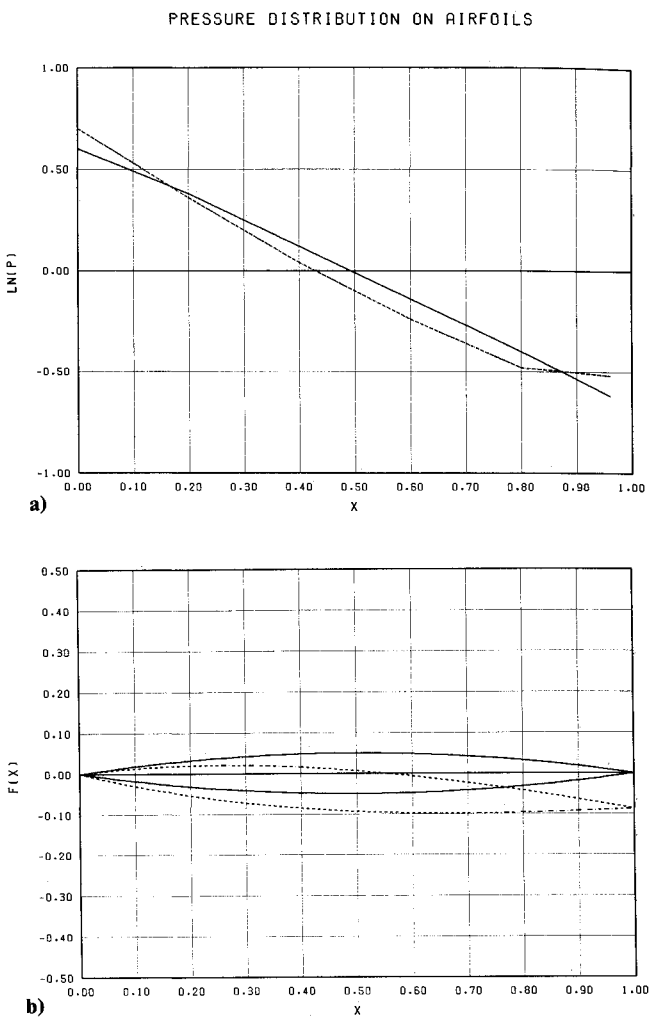

Fig. 4 a) Pressure distribution on 10% thick airfoil, uncambered at 0-deg angle of attack and cambered ($c = 0.1$) at 5-deg angle of attack at $M = 2$ along with b) respective bodies.

where

$$\frac{dw}{d\epsilon} = M^2 \sin 2\eta \frac{d\eta}{d\epsilon}$$

$$A = 1 + 0.2M^2(1+w) - (1+7/6w)(1+1/6w)$$

$$\frac{d\theta}{d\epsilon} = \frac{d\eta}{d\epsilon}\cos^2\theta\left\{-\frac{1}{\sin^2\eta}\right.$$

$$\times \frac{(M^2-1)\tan^2\eta - 1}{\left[\left(1+\frac{\gamma+1}{2}M^2\right)+\left(1+\frac{\gamma-1}{2}M^2\right)\tan^2\eta\right]}$$

$$+ \frac{2}{\left[\left(1+\frac{\gamma+1}{2}M^2\right)+\left(1+\frac{\gamma-1}{2}M^2\right)\tan^2\eta\right]^2}$$

$$\times\left[(M^2-1)\sec\eta\left(1+\frac{\gamma+1}{2}M^2\right)\right.$$

$$\left.+\left(1+\frac{\gamma-1}{2}M^2\right)\tan^2\eta\right]$$

$$\left.-[(M^2-1)\tan^2\eta - 1]\left(1+\frac{\gamma-1}{2}M^2\right)\sec^2\eta\right\} \qquad (24)$$

In the actual integration, Eqs. (20–23) are applied at the shock

$$\alpha = \beta \qquad (25)$$

At the body $\alpha = 0$, the appropriate equations are

$$X = 0, \qquad Y = f\frac{\partial\beta}{\partial\epsilon}, \qquad \theta = \frac{\partial f_\beta(\beta,\epsilon)}{\partial\epsilon}\cos^2\theta \qquad (26)$$

In writing Eq. (26), we revert to the general case in which many parameters are being considered. We can now simultaneously numerically integrate the nonlinear system and the variational equations. The calculation of the basic flow ($\epsilon = \epsilon_0$) is second-order accurate.[2] The calculation of the new flow is first-order in space and second-order in the parameters of interest. The calculation of the two flows is interleaved in that, after the flow along $\beta = \text{const}$ is computed by the base code, the parametric code then calculates the exact derivatives in order to obtain the perturbed flow.

As we have already mentioned, the method applies generally to many independently varying parameters. To accomplish this extension, we use Taylor's theorem to write

$$p_{\text{new}} = p_{\text{base}} + \sum_i \left(\frac{\partial p}{\partial \epsilon_i}\right)(\epsilon_i - \epsilon_{i0}) \qquad (27)$$

where ϵ_i represents the various parameters with the differential coefficients calculated holding α and β fixed. For example, if just thickness is considered and denoted by say ϵ, then at the body

$$p_{\text{new}} = p_{\text{base}} + \left(\frac{\partial p}{\partial \epsilon}\right)_{\alpha=0,\beta}(\epsilon - \epsilon_0) = p_{\text{base}}$$

$$+\left[\left(\frac{\partial p}{\partial \epsilon}\right)_{x,y=f} + \left(\frac{\partial p}{\partial y}\right)_{x,y=f}\left(\frac{\partial f}{\partial \epsilon}\right)\right](\epsilon - \epsilon_0) \qquad (28)$$

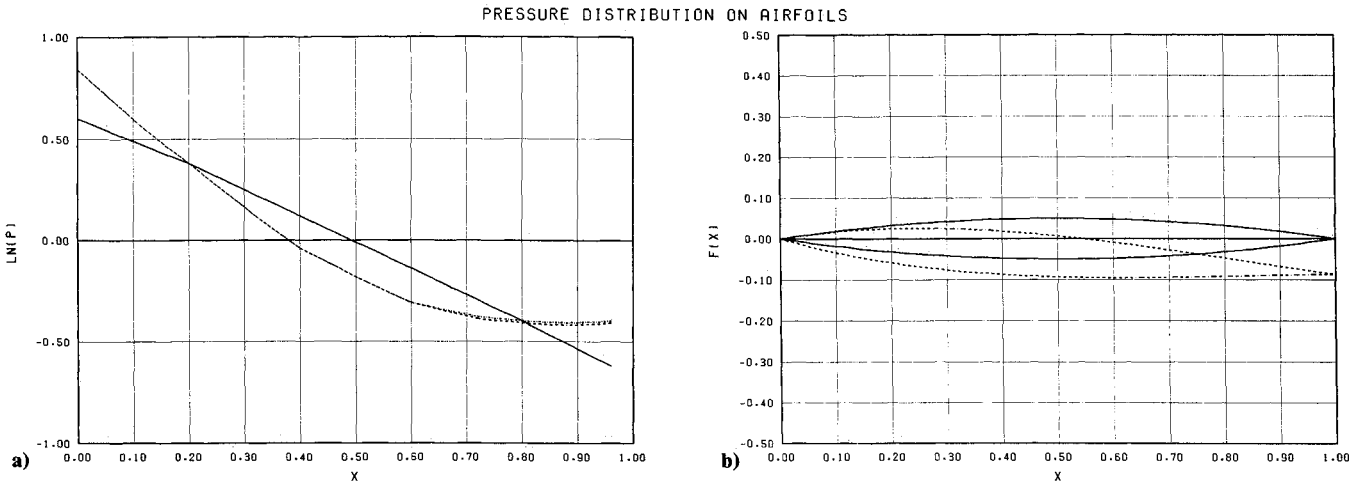

Fig. 5 a) Pressure distribution on 10% thick airfoil, uncambered at 0-deg angle of attack and cambered ($c = 0.2$) at 5-deg angle of attack at $M = 2$ along with b) respective bodies.

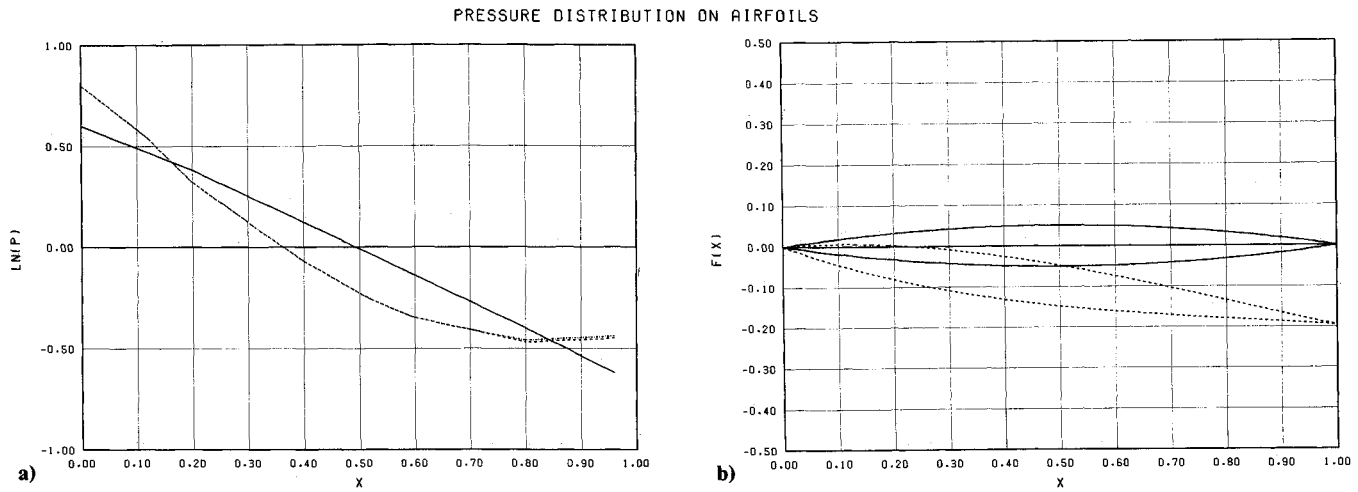

Fig. 6 a) Pressure distribution on 10% thick airfoil, uncambered at 0-deg angle of attack and cambered ($c = 0.2$) at 10-deg angle of attack at $M = 2$ along with b) respective bodies.

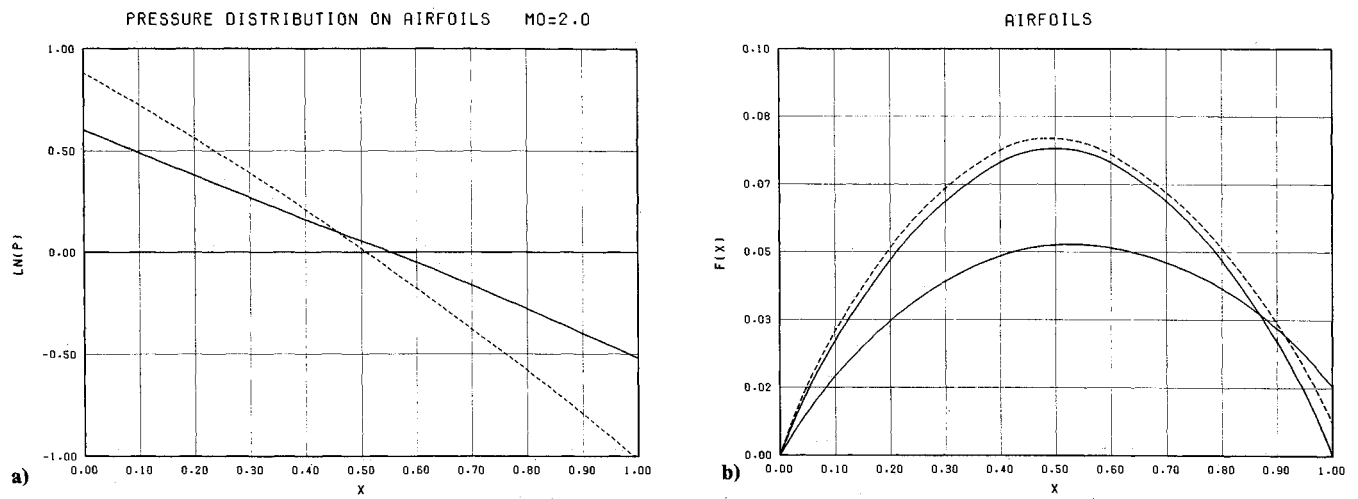

Fig. 7 a) Inverse case: pressure distribution on 10% and 12% airfoils, $M = 2$, along with b) generated bodies. Dashed airfoil is computed shape.

The second form of the equation is that obtained if variation in the physical plane is considered.

V. Results

In sample numerical calculations, we have taken for the wing surface contour function f a family of shapes given by

$$y = 2\epsilon x(1 - x) - x\tan\Delta + 10x(x - 1)[x - 1/2]c \quad (29)$$

Here ϵ is the thickness ratio based on chord, Δ is the mean chord angle of attack, and c is a scaling factor for the camber (shape) function.

Figure 3 shows the effect of changing just the thickness ($\Delta, c = 0$). Here we have plotted pressure distribution on the upper surface and the airfoil that, for aesthetics, has the lower surface plotted as a reflection of the upper surface. Note that

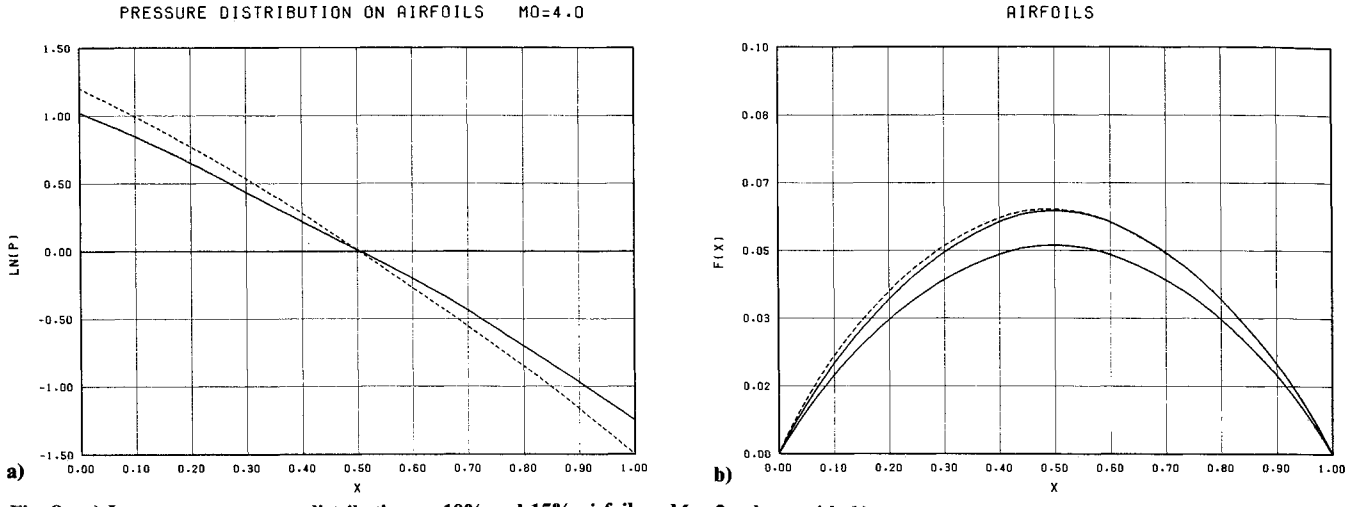

Fig. 8 a) Inverse case: pressure distribution on 10% and 15% airfoils, $M = 2$, along with b) generated bodies. Dashed airfoil is computed shape.

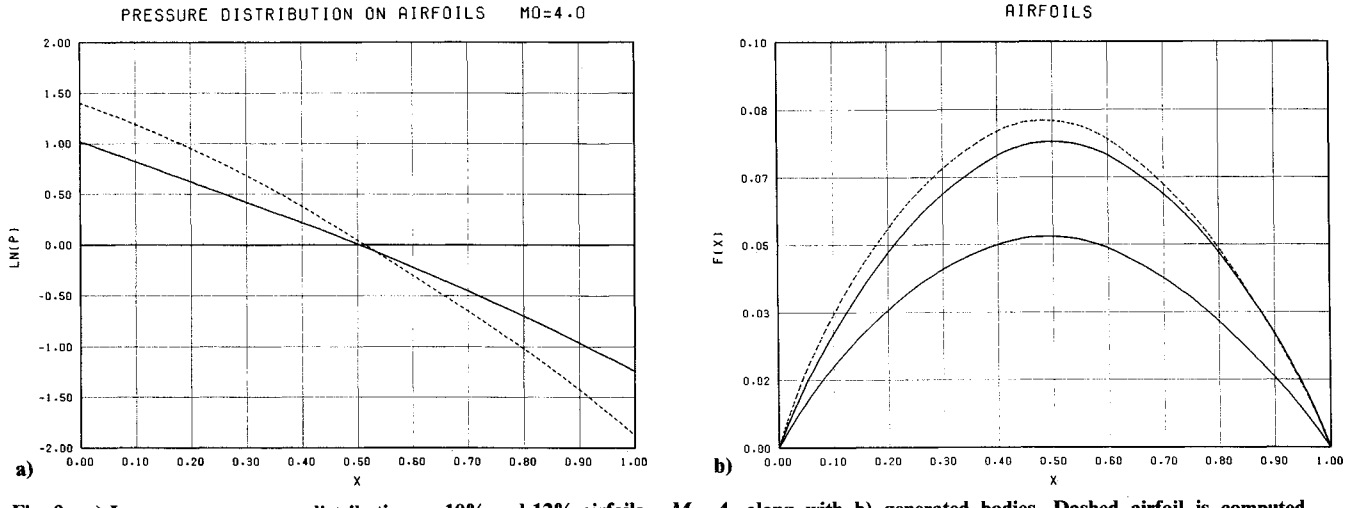

Fig. 9 a) Inverse case: pressure distribution on 10% and 12% airfoils, $M = 4$, along with b) generated bodies. Dashed airfoil is computed shape.

the method gives good agreement with the exact solution even when the new thickness is half again the base thickness.

More generally, we consider variations in all three parameters. Thus, the pressure relation at the body is

$$p_{\text{new}} = p_{\text{base}} + \left(\frac{\partial p}{\partial \epsilon}\right)_{\alpha=0,\beta} (\epsilon - \epsilon_0) + \left(\frac{\partial p}{\partial \theta}\right)_{\alpha=0,\beta} (\Delta - \Delta_0) + \left(\frac{\partial p}{\partial c}\right)_{\alpha=0,\beta} (c - c_0) \tag{30}$$

Figures 4–6 show the effect of changing various combinations of thickness, angle of attack, and camber. Here we see that, although the airfoil configurations are markedly different, there is very good agreement between the parametrically generated pressure distribution and the exact pressure distribution for the new airfoil.

VI. Inverse Case

The method that has been presented also works quite well in the inverse or design problem where the pressure on the body is known, but the shape of the body is unknown.

Using the Bernoulli equation and the perfect gas law one may show[1]

$$\mu = \sin^{-1}\left\{\left[\frac{\gamma-1}{2}\frac{\exp\left[\frac{\gamma-1}{\gamma}(s+\ell n\,\gamma p)\right]}{1+\frac{\gamma-1}{2}M^2-\exp\left[\frac{\gamma-1}{\gamma}(s+\ell n\,\gamma p)\right]}\right]^{1/2}\right\} \tag{31}$$

This, when differentiated, yields

$$\Psi - \frac{(\gamma-1)^2}{2\gamma}\frac{\left(1+\frac{\gamma-1}{2}M^2\right)\exp(w)}{\left[1+\frac{\gamma-1}{2}M^2-\exp(w)\right]^2\sin^2\mu}S = \frac{(\gamma-1)^2}{2\gamma}\frac{\left(1+\frac{\gamma-1}{2}M^2\right)\exp(w)}{\left[1+\frac{\gamma-1}{2}M^2-\exp(w)\right]^2\sin^2\mu}\frac{\mathrm{d}(\ell n\,p)}{\mathrm{d}\epsilon} \tag{32}$$

where

$$w = \frac{\gamma-1}{\gamma}(s+\ell n\,p)$$

We now use Eqs. (2), (5), (31), and (32) instead of Eqs. (2), (3), (5), and (6) at the body and do the calculation exactly as before. The results are presented in Figs 7–9. Notice that even for a 20% change in the log of the pressure (corresponding to a 50% increase in thickness), the difference between the exact airfoil shape and the computed shape is less than 4%.

VII. Conclusion

The method presented allows for an accurate parametric description of a path of solutions of a nonlinear system of partial differential equations. Although the method has been applied to supersonic flow over an airfoil, the generality of the method suggests that more versatile and efficient use of flow

computations may be achieved by modes changes to already existing flow codes.

References

[1]Lewis, T. S. and Sirovich, L., "Approximate and Exact Numerical Computation of Supersonic Flow Over an Airfoil," *Journal of Fluid Mechanics*, Vol. 112, 1981, pp. 265–282.

[2]Fong, J. and Sirovich, L., "Direct and Inverse Problem in Supersonic Axisymmetric Flow," *AIAA Journal*, Vol. 24, May 1986, pp. 852–854.